Available online at www.sciencedirect.com
ScienceDirect
European Journal of Mechanics B/Fluids 27 (2008) 202–217

Conservative approximation schemes of kinetic equations for chemical reactions

Maria Groppi [a], Peter Lichtenberger [b], Ferdinand Schürrer [b,*], Giampiero Spiga [a]

[a] *Dipartimento di Matematica, Università di Parma, V.le G.P. Usberti, 53/A, 43100 Parma, Italy*
[b] *Institut für Theoretische Physik, Computational Physics, Technische Universität Graz, Petersgasse 16, 8010 Graz, Austria*

Received 21 November 2006; received in revised form 4 April 2007; accepted 1 May 2007

Available online 18 May 2007

Abstract

Two approximate solutions to the kinetic equations for a gas mixture undergoing reversible bimolecular chemical reactions are presented. A conservative discrete ordinates method is compared to a conservative BGK approximation of the reactive Boltzmann equations. Features and performances of the two methods on both microscopic and macroscopic scales are investigated.

PACS: 05.20.Dd; 51.10.+y; 47.45.Ab; 47.70.Nd; 82.20.-w

Keywords: Boltzmann equation; BGK model; Chemical reaction; Discrete ordinates method

1. Introduction

The accurate numerical approximation of Boltzmann equations represents a challenging task and has been considered by many authors in the past decades. Just to mention a few, we recall here the pioneering work by Nordsieck's group [1] based on Monte Carlo techniques, finite difference approaches [2,3], spectral methods [4], Direct Simulation Monte Carlo calculations [5], as well as discrete and semi-discrete models [6–8]. The main problem in the numerical solution is the evaluation of the collision integrals. The difficulties become bigger if inelastic interactions, due for instance to chemical reactions and internal energy levels, are taken into account, since the collision part of the kinetic equations becomes much heavier. An accurate method for the calculation should preserve the conservation laws at any step. On this basis, discrete velocity models and semicontinuous models have been constructed to simulate Boltzmann equations in a conservative way [6–11].

The discrete ordinates method introduced in [12,13] by Tcheremissine, which is based on a discretization of the momentum space, overcomes a lot of shortfalls associated to other methods. It is designed to be conservative in every single collision, thus ensuring the fulfillment of the conservation laws at the macroscopic level. An extension to guarantee that the collision operator becomes zero in the case of equilibrium is presented in [14]. The method does

* Corresponding author. Tel.: +43 (316) 873 8177; fax: +43 (316) 873 8677.
E-mail addresses: maria.groppi@unipr.it (M. Groppi), lichtenb@itp.tugraz.at (P. Lichtenberger), schuerrer@itp.tugraz.at (F. Schürrer), giampiero.spiga@unipr.it (G. Spiga).

0997-7546/$ – see front matter
doi:10.1016/j.euromechflu.2007.05.001

not impose any limitation on the choice of impact parameters (compared to discrete velocity methods) or molecular potentials [15] and requires no symmetries of the distribution function (compared to semicontinuous approaches). Although it does not assume symmetries, the method can be easily adapted to exploit them, by reducing the effective dimension of the problem [16]. A good overview of the method, including extensions to inert mixtures of gases [16] and internal degrees of freedom [17], can be found in [18].

This discrete ordinates method was designed to be of low computational complexity right from the beginning, in order to allow the study of space-dependent problems of reasonable size in more than one spatial dimension. Analysis of the method was, therefore, mostly focused on hydrodynamic fields, namely moments of the distribution functions. In contrast, we intend to use it here for a deeper investigation of the microscopic level.

In this paper we extend Tcheremissine's method [18] to Boltzmann-like equations describing also bimolecular reversible chemical reactions like $A^1 + A^2 \rightleftharpoons A^3 + A^4$, and test its performance on space-homogeneous problems by comparison to a consistent reactive BGK approximation recently proposed by Groppi and Spiga [19] for the same process. The so-called BGK equations [20,21] constitute a well-known model of the nonlinear Boltzmann equation and a simpler tool of investigation, in particular for reacting gaseous flows. The BGK model considered here, for the reactive Boltzmann equations developed by Rossani and Spiga [22], is based on the simple idea of introducing only one BGK collision operator for each species. It is conservative in the sense that it guarantees the same rate of transfer for mass, momentum and total energy of the Boltzmann level, and thus reproduces exactly macroscopic conservation laws and kinetic equilibria. On the other hand, such a useful simplified model needs validation against actual accurate calculations at the Boltzmann level. The comparison between the discrete ordinates and the BGK approximations shows significant differences at the level of far-from-equilibrium distribution functions and emphasizes the power of discrete ordinates method as a proper tool of investigation of the microscopic level. Simultaneously, the present analysis confirms the reliability of a BGK approach, especially with respect to the macroscopic observable fields, when used within its limits of validity.

The paper is organized as follows. In Section 2 the Boltzmann equations for a bimolecular chemical reaction are described. The conservative discrete ordinates method for their accurate numerical solution is presented in Section 3. In Section 4 the reactive BGK approximation is recalled. Finally, the results of the comparison between the two considered methods are presented in Section 5 and some concluding remarks are given in Section 6.

2. Boltzmann equations for chemically reacting gases

We consider a chemically reactive gas of N_S components. Every species A^s is characterized by its internal energy E_s and particle mass m^s. The basic process considered is the binary encounter of two molecules of species A^i and A^j resulting in two molecules A^k and A^l:

$$A^i + A^j \to A^k + A^l. \tag{1}$$

Since not only elastic collisions but also chemical reactions are taken into account, the species of the involved particles can change, indicated by $(i, j) \to (k, l)$.

The gas kinetic state of a species A^s is given by its distribution function $f^s(\boldsymbol{p}, \boldsymbol{x}, t)$ depending on momentum $\boldsymbol{p}$, position $\boldsymbol{x}$ and time t. The extended kinetic equations of Boltzmann type for distribution functions $f^i(\boldsymbol{p}, \boldsymbol{x}, t)$ of the described chemically reacting mixture read

$$\frac{\partial f^i(\boldsymbol{p}, \boldsymbol{x}, t)}{\partial t} + \frac{\boldsymbol{p}}{m^i} \cdot \frac{\partial f^i(\boldsymbol{p}, \boldsymbol{x}, t)}{\partial \boldsymbol{x}} = C^i[f](\boldsymbol{p}) \tag{2}$$

for $i = 1, \ldots, N_S$, with the collision operators

$$C^i[f](\boldsymbol{p}) = \sum_{j=1}^{N_S} C_{ij}^{\mathrm{EL}}\big[f^i, f^j\big](\boldsymbol{p}) + \sum_{\mathbb{I}_{\mathrm{CH}}^i} C_{ij}^{kl}\big[f^i, f^j, f^k, f^l\big](\boldsymbol{p}). \tag{3}$$

For the sake of a compact notation, we introduce $f = (f^1, \ldots, f^{N_S})$ as the set of all distribution functions. In contrast to the common notation, we use distribution functions f^s depending on momentum $\boldsymbol{p}$ rather than velocity. This will lead to a more concise representation of collision operators and discretization schemes. The operator $C^i[f]$ separates into the elastic scattering operators $C_{ij}^{\mathrm{EL}}(\boldsymbol{p})$ and the operators for chemical reactions $C_{ij}^{kl}(\boldsymbol{p})$. The set of indices $\mathbb{I}_{\mathrm{CH}}^i$

restricts the summation over j, k and l to all possible reaction combinations $(i, j) \to (k, l)$ with given i, representing actual chemical reaction.

We focus here on a mixture of four suitably numbered species undergoing a reversible bimolecular chemical reaction

$$A^1 + A^2 \rightleftharpoons A^3 + A^4. \tag{4}$$

For this problem in its simplest version a kinetic model has been proposed and investigated by Rossani and Spiga [22]. Nevertheless, the setup can be easily expanded to treat systems involving more than one bimolecular reactive process, or internal energy structures [23]. By introducing the sets of quadruples of indices representing the different species involved in a collision $(i, j) \to (k, l)$

$$\mathbb{D}_{\mathrm{EL}} = \big\{(i, j, k, l) \mid i, j, k, l \in \{1, \ldots, 4\} \wedge (i = k) \wedge (j = l)\big\}, \tag{5}$$

$$\mathbb{D}_{\mathrm{CH}} = \big\{(1, 2, 3, 4), (2, 1, 4, 3), (3, 4, 1, 2), (4, 3, 2, 1)\big\} \tag{6}$$

and their union

$$\mathbb{D}_{\mathrm{PROC}} = \mathbb{D}_{\mathrm{EL}} \cup \mathbb{D}_{\mathrm{CH}}, \tag{7}$$

we may define, for each index i, the corresponding sets of triplets $\mathbb{I}^i_{\mathrm{EL}}$, $\mathbb{I}^i_{\mathrm{CH}}$ and $\mathbb{I}^i_{\mathrm{PROC}}$, where the set $\mathbb{I}^i_\alpha$ is made up of the strings (j, k, l) for which (i, j, k, l) belongs to $\mathbb{D}_\alpha$. Then the collision operators $C^{\mathrm{EL}}_{ij}(\boldsymbol{p})$ and $C^{kl}_{ij}(\boldsymbol{p})$ in (3) can be merged into the common form

$$C^i\big[f^1, \ldots, f^4\big](\boldsymbol{p}) = \sum_{\mathbb{I}^i_{\mathrm{PROC}}} C^{kl}_{ij}[f](\boldsymbol{p}). \tag{8}$$

The unified operator

$$C^{kl}_{ij}(\boldsymbol{p}) = G^{kl}_{ij}(\boldsymbol{p}) - L^{kl}_{ij}(\boldsymbol{p}) \tag{9}$$

consists of gain and loss terms:

$$G^{kl}_{ij}(\boldsymbol{p}) = \int_{\mathbb{R}^3}\int_{\mathbb{S}^2} f^k(\boldsymbol{p}')\, f^l(\boldsymbol{q}')\, \mathcal{B}^{kl}_{ij}(g_{ij}, \boldsymbol{\Omega} \cdot \boldsymbol{\Omega}')\, \mathrm{d}\boldsymbol{\Omega}'\, \mathrm{d}\boldsymbol{q}, \tag{10}$$

$$L^{kl}_{ij}(\boldsymbol{p}) = \int_{\mathbb{R}^3}\int_{\mathbb{S}^2} f^i(\boldsymbol{p})\, f^j(\boldsymbol{q})\, \mathcal{B}^{kl}_{ij}(g_{ij}, \boldsymbol{\Omega} \cdot \boldsymbol{\Omega}')\, \mathrm{d}\boldsymbol{\Omega}'\, \mathrm{d}\boldsymbol{q}, \tag{11}$$

where $\boldsymbol{p}'$ and $\boldsymbol{q}'$ are post-collision momenta. We introduce $\boldsymbol{\Omega}$ ($\boldsymbol{\Omega}'$) as the direction of the relative velocity of the particles with momenta $\boldsymbol{p}$ ($\boldsymbol{p}'$) and $\boldsymbol{q}$ ($\boldsymbol{q}'$). The scattering kernels $\mathcal{B}^{kl}_{ij}$ are considered depending on the modulus g of the relative velocity of the incoming particles and on $\boldsymbol{\Omega} \cdot \boldsymbol{\Omega}'$ only, which is a typical assumption in kinetic theory and can be justified by symmetry considerations [24].

For the binary collision dynamics, we consider the general encounter $(i, j) \to (k, l)$ with momentum transition $(\boldsymbol{p}, \boldsymbol{q}) \to (\boldsymbol{p}', \boldsymbol{q}')$. By defining the total mass $M = m^i + m^j$ and the reduced mass $\mu^{ij} = m^i m^j / M$ in the common way, we introduce

$$\boldsymbol{P} = \boldsymbol{p} + \boldsymbol{q} = \boldsymbol{p}' + \boldsymbol{q}', \tag{12}$$

$$\boldsymbol{h}_{ij} = \frac{1}{M}\big(m^j \boldsymbol{p} - m^i \boldsymbol{q}\big), \tag{13}$$

$$\boldsymbol{h}'_{kl} = \frac{1}{M}\big(m^l \boldsymbol{p}' - m^k \boldsymbol{q}'\big), \tag{14}$$

as new coordinates. Here, $\boldsymbol{P}$ clearly denotes the total momentum. A quick calculation shows that $\boldsymbol{h}_{ij} = \mu^{ij} \boldsymbol{g}_{ij}$, with $\boldsymbol{g}_{ij}$ standing for the relative velocity.

The post-collision momenta are given by

$$\boldsymbol{p}' = \frac{m^k}{M}\boldsymbol{P} + h'_{kl}\boldsymbol{\Omega}', \tag{15}$$

$$\boldsymbol{q}' = \frac{m^l}{M}\boldsymbol{P} - h'_{kl}\boldsymbol{\Omega}', \tag{16}$$

with

$$h'_{kl} = \left[\frac{\mu^{kl}}{\mu^{ij}}\left(h_{ij}^2 - \mathcal{E}_{ij}^{kl}\right)\right]^{1/2} \tag{17}$$

under the condition $h_{ij}^2 \geqslant \mathcal{E}_{ij}^{kl}$, where we introduce $\mathcal{E}_{ij}^{kl} = 2\mu^{ij}E_{ij}^{kl}$ with $E_{ij}^{kl} = E_k + E_l - E_i - E_j$, the energy yield of a single reactive collision. Therefore, $E_{ij}^{kl} = -E_{kl}^{ij}$ links the exo- and the endothermic reaction energy.

The Jacobian of the transformation from pre- to post-collision momentum coordinates is given by

$$\mathrm{d}\boldsymbol{p}\,\mathrm{d}\boldsymbol{q}\,\mathrm{d}\boldsymbol{\Omega}' = \frac{\mu^{ij}}{\mu^{kl}}\frac{h_{ij}}{h'_{kl}}\,\mathrm{d}\boldsymbol{p}'\,\mathrm{d}\boldsymbol{q}'\,\mathrm{d}\boldsymbol{\Omega}. \tag{18}$$

Additionally, we assume the microreversibility of the reactive scattering kernel as

$$\mu^{ij}h_{ij}\mathcal{B}_{kl}^{ij}(g_{ij}, \boldsymbol{\Omega}\cdot\boldsymbol{\Omega}') = \mu^{kl}h'_{kl}\mathcal{B}_{ij}^{kl}(g'_{kl}, \boldsymbol{\Omega}'\cdot\boldsymbol{\Omega}), \tag{19}$$

derived from the symmetry of the Schrödinger (or Liouville) equation under time reversal [25], and the symmetry relations $\mathcal{B}_{ij}^{kl}(g, \boldsymbol{\Omega}\cdot\boldsymbol{\Omega}') = \mathcal{B}_{ji}^{lk}(g, \boldsymbol{\Omega}\cdot\boldsymbol{\Omega}') = \mathcal{B}_{ij}^{kl}(g, -\boldsymbol{\Omega}\cdot\boldsymbol{\Omega}')$ resulting from obvious exchange properties. All of these facts have been taken into account in Eqs. (10)–(11).

We refer the interested reader to the paper of Rossani and Spiga [22] for more technical details. However, it is easy to see that the collision operator (8) is conservative in total particle number, mass, momentum and energy. This well-known fact is represented mathematically by

$$\sum_{\mathbb{D}_{\mathrm{PROC}}}\int_{\mathbb{R}^3} C_{ij}^{kl}[f](\boldsymbol{p})\,\mathrm{d}\boldsymbol{p} = 0, \tag{20}$$

$$\sum_{\mathbb{D}_{\mathrm{PROC}}}\int_{\mathbb{R}^3} m^i C_{ij}^{kl}[f](\boldsymbol{p})\,\mathrm{d}\boldsymbol{p} = 0, \tag{21}$$

$$\sum_{\mathbb{D}_{\mathrm{PROC}}}\int_{\mathbb{R}^3} \boldsymbol{p}C_{ij}^{kl}[f](\boldsymbol{p})\,\mathrm{d}\boldsymbol{p} = \boldsymbol{0}, \tag{22}$$

$$\sum_{\mathbb{D}_{\mathrm{PROC}}}\int_{\mathbb{R}^3} E^i(\boldsymbol{p})C_{ij}^{kl}[f](\boldsymbol{p})\,\mathrm{d}\boldsymbol{p} = 0, \tag{23}$$

where $E^i(\boldsymbol{p})$ is the total energy (kinetic plus internal) for a particle of species i and momentum $\boldsymbol{p}$

$$E^i(\boldsymbol{p}) = \frac{p^2}{2m^i} + E_i. \tag{24}$$

In particular, it was shown by Rossani and Spiga [22] that not only the total particle number is conserved by the collision operator $\{C^i\}$, but also some independent combinations of particle numbers $n^s + n^r$ involving both reactants and products, for instance those with $(r, s) = (1, 3), (1, 4), (2, 4)$. Correspondingly, we get seven exact non-closed macroscopic conservation equations, and a seven-parameter family of Maxwellians

$$\mathcal{M}^i(\boldsymbol{p}) = \frac{n^i}{(2m^i\pi KT)^{3/2}}\exp\left[-\frac{1}{2m^iKT}\left(\boldsymbol{p} - m^i\mathbf{u}\right)^2\right], \quad i = 1, \ldots, 4, \tag{25}$$

as collision equilibria with equilibrium densities bound together by the well known mass action law of chemistry

$$\frac{n^1n^2}{n^3n^4} = \left(\frac{m^1m^2}{m^3m^4}\right)^{3/2}\exp\left(\frac{E_{12}^{34}}{KT}\right). \tag{26}$$

All moments of the distribution functions, including particle number density n, mass velocity $\mathbf{u}$, temperature T, viscous stress tensor $\mathbf{p}$ and heat flux vector $\mathbf{q}$, both global and for single species, are defined in the standard way and may be found in [19]. Moreover, a strict entropy inequality for relaxation to equilibrium has also been established in terms of the H-functional [22]

$$H = \sum_{i=1}^{4} \int_{\mathbb{R}^3} f^i \log f^i \,\mathrm{d}\boldsymbol{p}. \tag{27}$$

3. Numerical approximation: the Discrete Ordinates Method (DOM)

For a numerical simulation of systems described by the Boltzmann equation (2), we present a numerical scheme based on a discretization of momentum space. To this end, we follow closely a strategy introduced by Tcheremissine [13] and extended to inert mixtures by Raines [16] and to internal energy levels by Tcheremissine [17], making it a reasonable choice for the application to chemical reactions.

As a first step, a discrete uniform momentum grid $\mathcal{P} = \{\boldsymbol{p}^1, \ldots, \boldsymbol{p}^{N_0}\}$ of N_0 points $\boldsymbol{p}^\tau$ (with constant spacing in each direction) on a limited domain $\mathbb{V}$ of the momentum space with volume V is introduced.

By using Dirac delta functions, the distribution functions can be approximated by

$$f^i(\boldsymbol{p}^*) = \frac{V}{N_0} \sum_{\tau=1}^{N_0} f^i_\tau \delta\big(\boldsymbol{p}^* - \boldsymbol{p}^\tau\big), \tag{28}$$

and gain term (10) and loss term (11) take the form

$$G^{kl}_{ij}(\boldsymbol{p}^*) = \frac{V}{N_0} \sum_{\tau=1}^{N_0} G^{kl}_{ij,\tau} \delta\big(\boldsymbol{p}^* - \boldsymbol{p}^\tau\big), \tag{29}$$

$$L^{kl}_{ij}(\boldsymbol{p}^*) = \frac{V}{N_0} \sum_{\tau=1}^{N_0} L^{kl}_{ij,\tau} \delta\big(\boldsymbol{p}^* - \boldsymbol{p}^\tau\big) \tag{30}$$

for $i \in \{1, \ldots, N_S\}$. Inserting (28), (29) and (30) into the Boltzmann equation (2) leads to a set of Boltzmann equations for the discretized distribution functions:

$$\frac{\partial f^i_\tau}{\partial t} + \frac{\boldsymbol{p}^\tau}{m^i} \cdot \frac{\partial f^i_\tau}{\partial \boldsymbol{x}} = \sum_{\mathbb{I}^i_{\mathrm{PROC}}} \big[G^{kl}_{ij,\tau} - L^{kl}_{ij,\tau}\big] \tag{31}$$

for $i \in \{1, \ldots, N_S\}$ and $\tau \in \{1, \ldots, N_0\}$.

Following [14,17] we consider the integral operator

$$Q[\phi] = \sum_{\mathbb{D}_{\mathrm{PROC}}} \int_{\mathbb{R}^3} \int_{\mathbb{R}^3} \int_{\mathbb{S}^2} \phi(\boldsymbol{p}, \boldsymbol{q}) \big[f^c(\boldsymbol{p}') f^d(\boldsymbol{q}') - f^a(\boldsymbol{p}) f^b(\boldsymbol{q})\big] \mathcal{B}^{cd}_{ab}(g_{ab}, \boldsymbol{\Omega} \cdot \boldsymbol{\Omega}') \,\mathrm{d}\boldsymbol{p}\,\mathrm{d}\boldsymbol{q}\,\mathrm{d}\boldsymbol{\Omega}' \tag{32}$$

to obtain the coefficients $G^{kl}_{ij,\tau}$ and $L^{kl}_{ij,\tau}$ dependent on f^i_τ so that the conservations (20)–(23) are fulfilled by the discretized equation (31) too. Applying it to $\phi = \delta(\boldsymbol{p}^* - \boldsymbol{p})\delta^{ij}_{kl}$ with $\delta^{ij}_{kl} = \delta_{ia}\delta_{jb}\delta_{kc}\delta_{ld}$ results in the following representations of the gain term (10) and the loss term (11)

$$G^{kl}_{ij}(\boldsymbol{p}^*) = \frac{1}{4} Q\big[\delta(\boldsymbol{p}^* - \boldsymbol{p}')\delta^{kl}_{ij} + \delta(\boldsymbol{p}^* - \boldsymbol{q}')\delta^{lk}_{ji}\big], \tag{33}$$

$$L^{kl}_{ij}(\boldsymbol{p}^*) = \frac{1}{4} Q\big[\delta(\boldsymbol{p}^* - \boldsymbol{p})\delta^{ij}_{kl} + \delta(\boldsymbol{p}^* - \boldsymbol{q})\delta^{ji}_{lk}\big]. \tag{34}$$

In the following step, these eight-fold integrals are transformed into a sum. To this end, a lattice of N_L points distributed over the domain $\mathbb{V}^2 \times \mathbb{S}^2$ is constructed. Each point of the lattice indexed by ν consists of two momenta $\boldsymbol{p}_\nu \in \mathcal{P}$ and $\boldsymbol{q}_\nu \in \mathcal{P}$, and a direction $\boldsymbol{\Omega}'_\nu = (\chi_\nu, \phi_\nu)$ with $\cos\chi_\nu = \boldsymbol{\Omega}_\nu \cdot \boldsymbol{\Omega}'_\nu$. The numerical approximation of the integral operators (33) and (34) reads

$$G_{kl}^{ij}(\boldsymbol{p}^*) = \frac{V^2\pi^2}{N_L}\sum_{\nu=1}^{N_L} B_\nu^{ijkl}\big[\delta(\boldsymbol{p}^* - \boldsymbol{p}'_\nu) + \delta(\boldsymbol{p}^* - \boldsymbol{q}'_\nu)\big], \tag{35}$$

$$L_{kl}^{ij}(\boldsymbol{p}^*) = \frac{V^2\pi^2}{N_L}\sum_{\nu=1}^{N_L} B_\nu^{ijkl}\big[\delta(\boldsymbol{p}^* - \boldsymbol{p}_\nu) + \delta(\boldsymbol{p}^* - \boldsymbol{q}_\nu)\big], \tag{36}$$

with

$$B_\nu^{ijkl} = \big[f^k(\boldsymbol{p}'_\nu) f^l(\boldsymbol{q}'_\nu) - f^i(\boldsymbol{p}_\nu) f^j(\boldsymbol{q}_\nu)\big] \mathcal{B}_{kl}^{ij}(g_{ij}, \chi_\nu) \Theta_{\mathbb{V}_{\boldsymbol{p}'}\times\mathbb{V}_{\boldsymbol{q}'}} \sin\chi_\nu, \tag{37}$$

where $\sin\chi_\nu$ comes from $\mathrm{d}\boldsymbol{\Omega}' = \sin\chi\,\mathrm{d}\chi\,\mathrm{d}\varphi$ and the characteristic function $\Theta_{\mathbb{V}_{\boldsymbol{p}'}\times\mathbb{V}_{\boldsymbol{q}'}}$ yields $\Theta = 1$ for $\boldsymbol{p}' \in \mathbb{V} \wedge \boldsymbol{q}' \in \mathbb{V}$ and $\Theta = 0$ otherwise.

It is very important to note that the numerical evaluation of the gain and loss terms must be carried out in a synchronous manner, meaning that the same integration lattices must be used in (35) and (36).

In general, $\boldsymbol{p}'_\nu$ and $\boldsymbol{q}'_\nu$ are not elements of the momentum grid, which means that for the numerical evaluation of (35) and (36) two problems arise: first, a procedure must be found to handle the delta functions $\delta(\boldsymbol{p}^* - \boldsymbol{p}'_\nu)$ and $\delta(\boldsymbol{p}^* - \boldsymbol{q}'_\nu)$ and, second, one must decide which values the distribution functions $f^k(\boldsymbol{p}'_\nu)$ and $f^l(\boldsymbol{q}'_\nu)$ take on in this case.

For this purpose we approximate the pair of delta functions in the gain term (35) by a linear combination of two pairs of delta functions with singularities matching the momentum grid [13]:

$$\delta(\boldsymbol{p}^* - \boldsymbol{p}'_\nu) + \delta(\boldsymbol{p}^* - \boldsymbol{q}'_\nu) \approx (1 - r_\nu)\big[\delta\big(\boldsymbol{p}^* - \boldsymbol{p}_\nu^c\big) + \delta\big(\boldsymbol{p}^* - \boldsymbol{q}_\nu^c\big)\big] + r_\nu\big[\delta\big(\boldsymbol{p}^* - \boldsymbol{p}_\nu^s\big) + \delta\big(\boldsymbol{p}^* - \boldsymbol{q}_\nu^s\big)\big] \tag{38}$$

with $0 \leqslant r_\nu \leqslant 1$ and the additional condition

$$\boldsymbol{p}_\nu^c + \boldsymbol{q}_\nu^c = \boldsymbol{p}_\nu^s + \boldsymbol{q}_\nu^s = \boldsymbol{P}. \tag{39}$$

In this way, the conservation of particle number, mass and momentum is guaranteed. The coefficient r_ν can be determined by the conservation of energy

$$r_\nu = \frac{E'_\nu - E_\nu^c}{E_\nu^s - E_\nu^c} \tag{40}$$

with $E'_\nu = E^k(\boldsymbol{p}'_\nu) + E^l(\boldsymbol{q}'_\nu)$, $E_\nu^c = E^k(\boldsymbol{p}_\nu^c) + E^l(\boldsymbol{q}_\nu^c)$, $E_\nu^s = E^k(\boldsymbol{p}_\nu^s) + E^l(\boldsymbol{q}_\nu^s)$. The points of the momentum grid used in (38) are the pair of closest points $\boldsymbol{p}_\nu^c$ and $\boldsymbol{q}_\nu^c$ to $\boldsymbol{p}'_\nu$ and $\boldsymbol{q}'_\nu$ and a second suitable chosen pair $\boldsymbol{p}_\nu^s$ and $\boldsymbol{q}_\nu^s$ close to it, so that $0 \leqslant r_\nu \leqslant 1$ is true.

To evaluate B_ν^{ijkl}, we introduce the approximation [14]

$$f^k(\boldsymbol{p}'_\nu) f^l(\boldsymbol{q}'_\nu) \approx \big[f^k\big(\boldsymbol{p}_\nu^c\big) f^l\big(\boldsymbol{q}_\nu^c\big)\big]^{(1-r_\nu)}\big[f^k\big(\boldsymbol{p}_\nu^s\big) f^l\big(\boldsymbol{q}_\nu^s\big)\big]^{r_\nu}. \tag{41}$$

This ensures, by the definition of r_ν, that formula (41) becomes exact in the case of a Maxwellian distribution and that the integrand B_ν^{ijkl} vanishes, as for the non-discretized collision operator, in the case of equilibrium.

The coefficients $G_{ij,\tau}^{kl}$ and $L_{ij,\tau}^{kl}$ on the right-hand side of the discrete approximation (29) and (30) are obtained by a comparison of the coefficients of the delta functions in (35) and (36) with the coefficients in (29) and (30) by taking into account (38) and (41):

$$G_{ij,\tau}^{kl} = A\sum_\nu^{N_\nu}\big[(1 - r_\nu)\big(B^{ijkl}_{\boldsymbol{p}_\nu^c=\boldsymbol{p}^\tau} + B^{ijkl}_{\boldsymbol{q}_\nu^c=\boldsymbol{p}^\tau}\big) + r_\nu\big(B^{ijkl}_{\boldsymbol{p}_\nu^s=\boldsymbol{p}^\tau} + B^{ijkl}_{\boldsymbol{q}_\nu^s=\boldsymbol{p}^\tau}\big)\big], \tag{42}$$

$$L_{ij,\tau}^{kl} = A\sum_\nu^{N_\nu}\big[B^{ijkl}_{\boldsymbol{p}_\nu=\boldsymbol{p}^\tau} + B^{ijkl}_{\boldsymbol{q}_\nu=\boldsymbol{p}^\tau}\big], \tag{43}$$

where $A = V^2\pi^2\,N_0/N_L$ and $B^{ijkl}_{\boldsymbol{p}_\nu=\boldsymbol{p}^\tau} = B_\nu^{ijkl}\delta_{\boldsymbol{p}_\nu\boldsymbol{p}^\tau}$.

For the study of isotopic problems, the method presented for the general case without symmetries in momentum space can be simplified by using spherical coordinates for momenta and only discretizing the modulus of the momentum vector in the described way. The points of the integration lattice again consist of two momenta $\boldsymbol{p}_\nu = (p_r^\nu, p_\vartheta^\nu, p_\varphi^\nu)$

and $\boldsymbol{q}_\nu = (q_r^\nu, q_\vartheta^\nu, q_\varphi^\nu)$ and a direction $\boldsymbol{\Omega}'_\nu = (\chi_\nu, \phi_\nu)$, but now only p_r^ν and q_r^ν are grid points. The determination of $\boldsymbol{p}_\nu^c$, $\boldsymbol{q}_\nu^c$, $\boldsymbol{p}_\nu^s$ and $\boldsymbol{q}_\nu^s$ reduces to the determination of their radial components, their angular components need not be considered. For the approximation (38) again two pairs of close grid points are needed. In the case of spherical coordinates the determination of these points reduces to a one-dimensional problem. For the calculation of r_ν, Eq. (40) is still valid. It should be noted that different pairs of grid points need not be disjoint, i.e., they can share one point.

4. Reactive BGK equations

The numerical approximation by the discrete ordinates method of the reactive Boltzmann equations (2) will be compared in the next section with the solution of a consistent BGK approximation [19] for the same Boltzmann equations.

The BGK approximation to Eqs. (2) developed by Groppi and Spiga [19] in the spirit of Andries, Aoki and Perthame [26] leads to the equations

$$\frac{\partial f^i}{\partial t} + \frac{\boldsymbol{p}}{m^i} \cdot \frac{\partial f^i}{\partial \mathbf{x}} = \widetilde{C}^i[f] \equiv \nu_i \left(\mathcal{M}_i - f^i\right), \quad i = 1, \ldots, 4, \tag{44}$$

where $\mathcal{M}_i$ is a local Maxwellian with 5 disposable parameters $n_i, \mathbf{u}_i, T_i$,

$$\mathcal{M}_i(\mathbf{p}) = \frac{n_i}{(2\pi m^i K T_i)^{3/2}} \exp\left[-\frac{1}{2m^i K T_i}\left(\boldsymbol{p} - m^i \mathbf{u}_i\right)^2\right], \quad i = 1, \ldots, 4. \tag{45}$$

The factor ν_i is a (macroscopic) collision frequency, i.e. inverse collision time, independent of $\boldsymbol{p}$. The above auxiliary fields n_i, $\mathbf{u}_i$, T_i are determined from the corresponding actual moments of the distribution functions f^i (namely number density n^i, mass velocity $\mathbf{u}^i$ and temperature T^i of each component) by requiring that the exchange rates for mass, momentum and total (kinetic plus chemical) energy prescribed by (44) coincide with those deduced from the reactive Boltzmann equations (2), and described by Rossani and Spiga [22]. The resulting BGK model turns out to be a conservative approximation of the reactive Boltzmann equations (2), since it allows to reproduce exactly macroscopic conservation laws and equilibria. Analytical details and a discussion of the scheme may be found in [19].

The exchange rates for reactive BGK equations (44) are given by

$$\begin{aligned}
&\int_{\mathbb{R}^3} \widetilde{C}^i \,\mathrm{d}\boldsymbol{p} = \nu_i \left(n_i - n^i\right), \\
&\int_{\mathbb{R}^3} \boldsymbol{p}\, \widetilde{C}^i \,\mathrm{d}\boldsymbol{p} = \nu_i m^i \left(n_i \mathbf{u}_i - n^i \mathbf{u}^i\right), \\
&\int_{\mathbb{R}^3} \frac{p^2}{2m^i}\, \widetilde{C}^i \,\mathrm{d}\boldsymbol{p} = \nu_i \left[n_i \frac{3}{2} K T_i - n^i \frac{3}{2} K T^i + n_i \frac{1}{2} m^i u_i^2 - n^i \frac{1}{2} m^i \left(u^i\right)^2\right].
\end{aligned} \tag{46}$$

The corresponding exchange rates for mass, momentum and kinetic energy of each species for the Boltzmann equations (2) are much more complicated to compute, especially the chemical contributions, but they can be cast in closed analytical forms for Maxwellian molecules [19]. For the mechanical part we have [26,27]

$$\begin{aligned}
&\sum_{j=1}^{4} \int_{\mathbb{R}^3} C_{ij}^{\mathrm{EL}} \,\mathrm{d}\boldsymbol{p} = \mathbf{0}, \\
&\sum_{j=1}^{4} \int_{\mathbb{R}^3} \boldsymbol{p}\, C_{ij}^{\mathrm{EL}} \,\mathrm{d}\boldsymbol{p} = \sum_{j=1}^{4} \nu_{ij}^1 \mu^{ij} n^i n^j \left(\mathbf{u}^j - \mathbf{u}^i\right), \\
&\sum_{j=1}^{4} \int_{\mathbb{R}^3} \frac{p^2}{2m^i}\, C_{ij}^{\mathrm{EL}} \,\mathrm{d}\boldsymbol{p} = \sum_{j=1}^{4} \nu_{ij}^1 \frac{2\mu^{ij}}{m^i + m^j} n^i n^j \left[\frac{3}{2} K \left(T^j - T^i\right) \frac{1}{2} \left(m^j \mathbf{u}^j + m^i \mathbf{u}^j\right) \cdot \left(\mathbf{u}^j - \mathbf{u}^i\right)\right].
\end{aligned} \tag{47}$$

Such exchange rates turn out to depend on the microscopic collision frequencies (constant with respect to the impact speed g in our assumptions)

$$\nu_{ij}^k(g) = \nu_{ji}^k(g) = 2\pi \int_0^\pi \mathcal{B}_{ij}^{ij}(g,\chi)(1-\cos\chi)^k \sin\chi \,\mathrm{d}\chi, \quad k = 0, 1. \tag{48}$$

The analytical computation of the chemical contributions to $\{C^i\}$, again in a pseudo-Maxwellian assumption of g-independent chemical collision frequency

$$\nu_{12}^{34} = 2\pi \int_0^\pi \mathcal{B}_{12}^{34}(g,\chi)\sin\chi \,\mathrm{d}\chi, \tag{49}$$

can be made explicit in the case of slow chemical reactions [27] by assuming that the characteristic relaxation time for the chemical reaction is larger than the corresponding elastic relaxation time. Then we obtain

$$\begin{aligned}
&\int_{\mathbb{R}^3} C_{ij}^{kl}\,\mathrm{d}\boldsymbol{p} = \lambda^i \mathcal{S},\\
&\int_{\mathbb{R}^3} \boldsymbol{p}\, C_{ij}^{kl}\,\mathrm{d}\boldsymbol{p} = \lambda^i \mathcal{S} m^i \mathbf{u},\\
&\int_{\mathbb{R}^3} \frac{p^2}{2m^i} C_{ij}^{kl}\,\mathrm{d}\boldsymbol{p} = \lambda^i \mathcal{S}\left[\frac{1}{2}m^i u^2 + \frac{3}{2}(KT) - \frac{1-\lambda^i}{2}\,\frac{M-m^i}{M}\,E_{12}^{34}\right.\\
&\qquad\qquad \left. + \frac{M-m^i}{M}\,KT\,\frac{\left(E_{12}^{34}/(KT)\right)^{3/2}\mathrm{e}^{-E_{12}^{34}/(KT)}}{\Gamma\left(3/2, E_{12}^{34}/(KT)\right)}\right],
\end{aligned} \tag{50}$$

where λ_i are the stoichiometric coefficients ($\lambda_1 = \lambda_2 = -\lambda_3 = -\lambda_4 = 1$) and

$$\mathcal{S} = \nu_{12}^{34}\,\frac{2}{\sqrt{\pi}}\,\Gamma\left(\frac{3}{2}, \frac{E_{12}^{34}}{KT}\right)\left[n^3 n^4 \left(\frac{m^1 m^2}{m^3 m^4}\right)^{3/2} \mathrm{e}^{E_{12}^{34}/(KT)} - n^1 n^2\right], \tag{51}$$

with Γ denoting the incomplete gamma function [28].

Though the BGK approximation is rough, it is expected to give a good description, at least of the macroscopic evolution, if the 20 overall disposable parameters n_i, $\mathbf{u}_i$, T_i are chosen in such a way that the same exact exchange rates of the kinetic level are prescribed. It suffices to equate the right-hand sides of (46) with the sum of the corresponding right-hand sides of (47) and (50), which provides for given $\nu_i > 0$ a set of 20 uniquely and explicitly solvable linear algebraic equations for the 20 free parameters (functions of $\mathbf{x}$ and t) previously introduced. Such a choice implies in particular that the BGK equations (44) fulfil exactly the seven correct conservation laws. In addition, the BGK equations (44) share with the kinetic equations (2) the correct collision equilibrium (25), (26). The kinetic H-functional (27) has been numerically verified to decrease along solutions. A discussion on the proper choice of the collision frequencies ν_i, which measure the strength at which the model equations (44) push distributions towards equilibrium, may be found again in [19]. We quote here only the conclusions, based on a suitable counting of the actual average number of collisions taking place for each species, that suggest the choice

$$\begin{aligned}
\nu_1 &= \sum_{j=1}^4 \nu_{1j}^0 n^j + \frac{2}{\sqrt{\pi}}\Gamma\left(\frac{3}{2}, \frac{E_{12}^{34}}{KT}\right)\nu_{12}^{34} n^2,\\
\nu_2 &= \sum_{j=1}^4 \nu_{2j}^0 n^j + \frac{2}{\sqrt{\pi}}\Gamma\left(\frac{3}{2}, \frac{E_{12}^{34}}{KT}\right)\nu_{12}^{34} n^1,\\
\nu_3 &= \sum_{j=1}^4 \nu_{3j}^0 n^j + \frac{2}{\sqrt{\pi}}\Gamma\left(\frac{3}{2}, \frac{E_{12}^{34}}{KT}\right)\left(\frac{\mu^{12}}{\mu^{34}}\right)^{3/2} \mathrm{e}^{E_{12}^{34}/(KT)}\nu_{12}^{34} n^4,
\end{aligned} \tag{52}$$

$$\nu_4 = \sum_{j=1}^{4} \nu_{4j}^0 n^j + \frac{2}{\sqrt{\pi}}\Gamma\left(\frac{3}{2}, \frac{E_{12}^{34}}{KT}\right)\left(\frac{\mu^{12}}{\mu^{34}}\right)^{3/2} \mathrm{e}^{E_{12}^{34}/(KT)} \nu_{12}^{34} n^3.$$

The main advantage of the BGK equations is their much easier numerical implementation with respect to the actual Boltzmann reactive equations. As for any approximation, a comparison with "exact" results is essential as an accuracy test, as well as a clue for possible further improvements. Numerical tests performed so far on macroscopic parameters have turned out to be quite satisfactory, but the need for comparisons at the kinetic level of the distribution functions, for which the approximation cannot be expected to be good for initial and intermediate times, was indeed one of the motivations of the present work.

5. Numerical simulations and comparison

We present some numerical simulations of the kinetic models discussed above, with the aim of pointing out peculiarities and differences between the two approaches. We stick to space homogeneous problems and consider the BGK results presented by Groppi and Spiga [19] as a first comparison with the DOM approximation. For this reason the numerical values used for the test are taken from [19] and, therefore, are to be considered dimensionless and corresponding to an arbitrary scale. They have been chosen for illustrative purposes, without any reference to an actual specific problem.

5.1. Cross-section

So far the scattering kernels $\mathcal{B}_{ij}^{kl}$ have not been specified. The BGK method uses collision frequencies, which are obtained by integrating the scattering kernels with respect to the deflection angle. Consequently, there exists no one-to-one relation between collision frequencies and scattering kernels.

We assume that the scattering kernel $\mathcal{B}_{ij}^{kl}$ is based on the well-known Maxwellian cross section

$$\mathcal{B}_{ij}^{ij}(g_{ij}, \boldsymbol{\Omega} \cdot \boldsymbol{\Omega}') = \kappa_{ij} = const. \tag{53}$$

for elastic collisions, with $\kappa_{ij} = \kappa_{ji}$. In the case of chemical reactions, we may assume, without loss of generality, that the reaction is endothermic from the left to the right, namely $E_{12}^{34} > 0$, and postulate

$$\mathcal{B}_{12}^{34}(g_{12}, \boldsymbol{\Omega} \cdot \boldsymbol{\Omega}') = \kappa_{12}^{34} \Theta\left[{g_{12}}^2 - \mathcal{E}_{12}^{34}/\left(\mu^{12}\right)^2\right], \tag{54}$$

so that by microreversibility (19) we get

$$\mathcal{B}_{34}^{12}(g_{34}, \boldsymbol{\Omega} \cdot \boldsymbol{\Omega}') = \kappa_{34}^{12} \frac{g_{12}'}{g_{34}} \tag{55}$$

with

$$\left(\mu^{12}\right)^2 \kappa_{12}^{34} = \left(\mu^{34}\right)^2 \kappa_{34}^{12}, \tag{56}$$

and $\kappa_{ij}^{kl} = \kappa_{ji}^{lk}$ as scattering strength. The assumption in (53) and (54) that $\mathcal{B}_{ij}^{kl}$ is independent of the deflection angle, results in a simple relation between ν_{ij} and κ_{ij}. Definition (48) for the elastic collision frequencies gives

$$\nu_{ij}^k = 4\pi \kappa_{ij} \tag{57}$$

for $k = 0, 1$, and definition (49) results in

$$\nu_{12}^{34} = 4\pi \kappa_{12}^{34} \tag{58}$$

for the chemical collision frequency.

5.2. Numerics

For the DOM method the lattice points must be chosen uniformly distributed over the integration domain to ensure that the discrete representation of the gain (35) and the loss (36) terms converge to the respective continuous forms as $N_L \to \infty$.

In this work, we use the Korobov–Hlawka lattice rule [29,30] already used in the original work of Tcheremissine [12]. We generate more than one lattice with N_L elements and alternate them during the time evolution in order to reduce the probability of systematic numerical errors [31,32]. For the simulations in this work, we typically use 24 integration lattices with $N_L \approx 4000$ integration points each.

For both the DOM and the BGK methods, the momentum space is discretized on the interval $[0, 60]$ by 120 equivalent subintervals. Integrations to determine moments of distribution functions are performed by applying the midpoint rule. The approximation of the reactive BGK equations (44) involves at each time step the explicit solution of the linear system giving the auxiliary variables in terms of the actual moments of distribution functions, and the numerical solution of systems of ODEs, which have been computed by adaptive Runge–Kutta methods.

Based on our numerical setup, we found a factor of 50 to 100 between the computational cost of the BGK implementation and the DOM code in favor of the BGK method. General statements on the DOMs computational cost are difficult to give, as N_L and, therefore, the computational effort for the evaluation of the collision operator can be chosen independently of the phase-space discretization. However, the accuracy of the evaluation of the collision integral affects the time evolution in a nontrivial way. Typically, a less accurate numerical integration of the collision operator implies smaller time-steps.

5.3. Basic setup

For all studies, we assume a reacting gas mixture of four species defined by the masses

$$m^1 = 11.7, \quad m^2 = 3.6, \quad m^3 = 3.7, \quad m^4 = 7.3. \tag{59}$$

The elastic collisions between the components are characterized by the collision frequencies

$$\nu_{ij} = \begin{pmatrix} 0.3 & 0.4 & 0.1 & 0.4 \\ 0.4 & 0.3 & 0.4 & 0.6 \\ 0.1 & 0.4 & 0.3 & 0.2 \\ 0.4 & 0.6 & 0.2 & 0.4 \end{pmatrix}. \tag{60}$$

These parameters are fixed throughout this work, as well as the fact that the reaction $A^1 + A^2 \to A^3 + A^4$ is always the endothermic one (i.e. $E_{12}^{34} > 0$), albeit with different collision frequencies ν_{12}^{34} and energy thresholds E_{12}^{34}. This setup is nearly identical to the one used in the previous paper [19]. The only difference is that we now have $\nu_{ij}^0 = \nu_{ij}^1 = \nu_{ij}$.

5.4. Simulations

For a first validation of the BGK model and the kinetic DOM approach, we choose a gas mixture with initial conditions given by Maxwellian distributions with the following macroscopic parameters

$$\begin{aligned} &n^1(0) = 10, \quad n^2(0) = 12, \quad n^3(0) = 14, \quad n^4(0) = 13, \\ &T^1(0) = 4.0, \quad T^2(0) = 4.3, \quad T^3(0) = 3.7, \quad T^4(0) = 3.5. \end{aligned} \tag{61}$$

The collision frequency ν_{12}^{34} describing the rate of chemical reactions is

$$\nu_{12}^{34} = 0.01 \tag{62}$$

and, therefore, one order of magnitude smaller than all the elastic collision frequencies ν_{ij}, namely in the range of validity of the BGK approximation. The energy difference between reactants and products of the chemical reaction is $E_{12}^{34} = 10$.

In Fig. 1 the relaxation process is depicted in terms of the time evolution of temperatures and number densities. Differences between the two applied models are hardly visible. The numerical evaluation of the differences reveals that the relative error is in the range of 10^{-3} and, equally important, tends to zero in the case of equilibrium.

Next, we use the same data to demonstrate the numerical behavior of the DOM method by evaluating the collision term $C^i[f](\boldsymbol{p})$ for the Maxwellian distributions defined by (61). We estimate the quality of the evaluation of the collision operator at a certain N_L by performing the calculation with different integration lattices as described in 5.2. With every single lattice, we determine a DOM approximation of the collision operator and the change of macroscopic

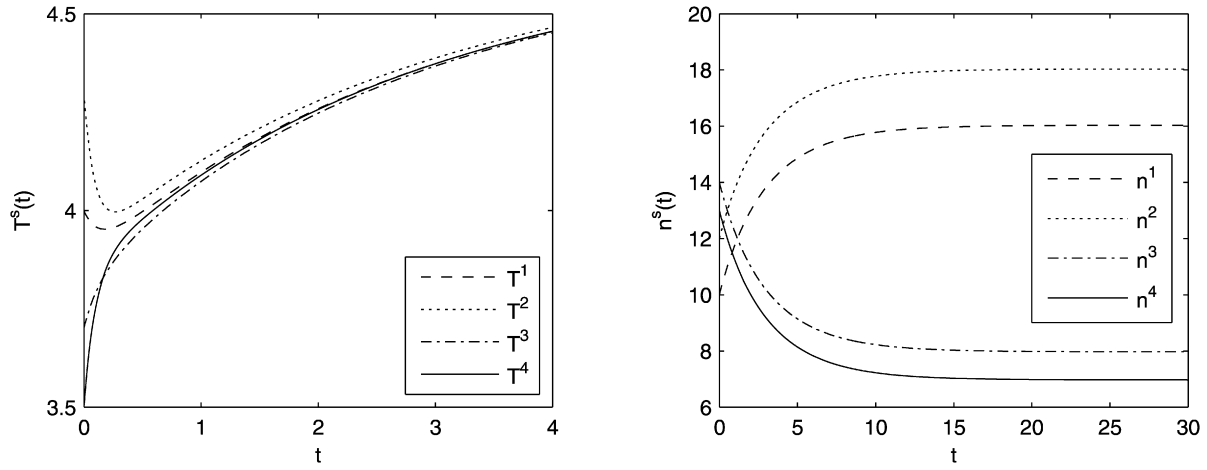

Fig. 1. Time evolution of temperatures T^s (left plot) and number densities n^s (right plot) The solutions obtained by the BGK and the DOM method cannot be distinguished in these pictures.

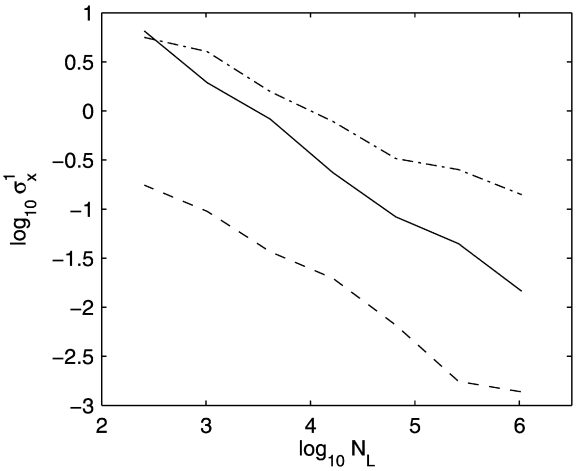

Fig. 2. Relative standard deviation of the change in energy σ_E^1 (solid line) and number density σ_n^1 (dashed line) and σ_f^1 (dash-dotted line), as defined in Eq. (63) for species 1.

quantities of the different species. The statistics of the different results give us an estimate for the variance of a single result.

In addition to the standard deviation of the change of kinetic energy σ_E^i and number density σ_n^i, as representative values of the quality of the DOM method in terms of macroscopic quantities, we introduce

$$\sigma_f^i = \frac{\max_p(\mathrm{var}(p^2 C^i))}{\max_p(|p^2 C^i|)} \tag{63}$$

as a measure for the quality concerning the distribution itself. The behavior of these standard deviations as function of N_L for species 1 is depicted in Fig. 2, showing that macroscopic quantities converge faster (exponent of the convergence rate $\alpha_{\mathrm{macro.}} \approx 0.7$) than the collision operator ($\alpha_{\mathrm{micro.}} \approx 0.4$) itself. This is obvious since the inaccuracy, as illustrated in Fig. 3, of the collision operator decreases, at least to some degree, when determining macroscopic quantities. The results for the other species do not deviate significantly in their convergence rate.

To demonstrate the limits of the BGK-model, we alter the reactive collision frequency to

$$\nu_{12}^{34} = 1.0, \tag{64}$$

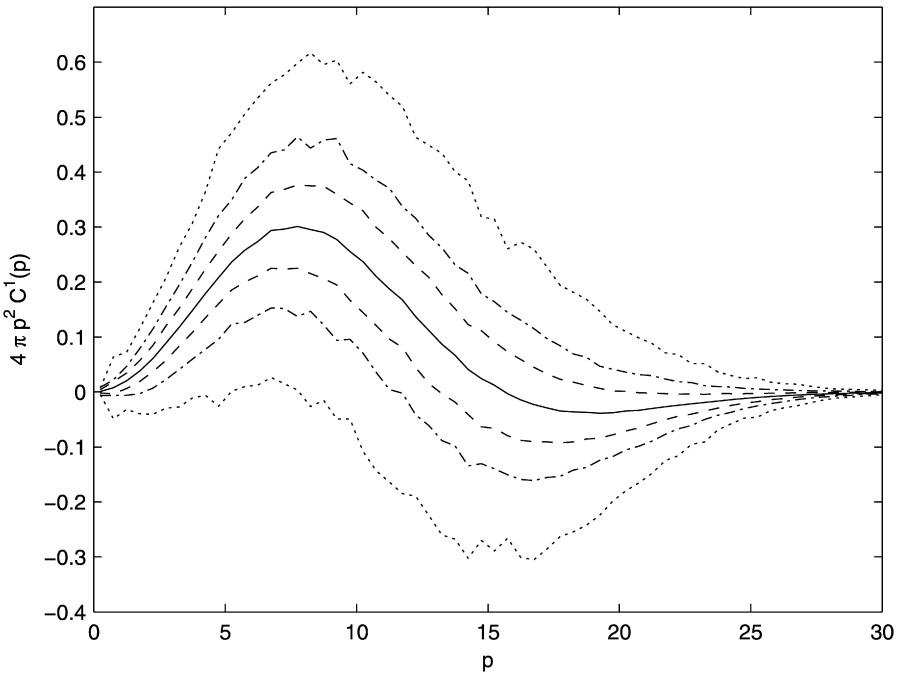

Fig. 3. Collision operator multiplied by $4\pi p^2$ for species 1 at $t = 0$ (solid line) and the confidence band spanned by the standard deviation at $N_L = 1000$ (dotted line), 4000 (dash-dotted line) and 16 000 points (dashed line).

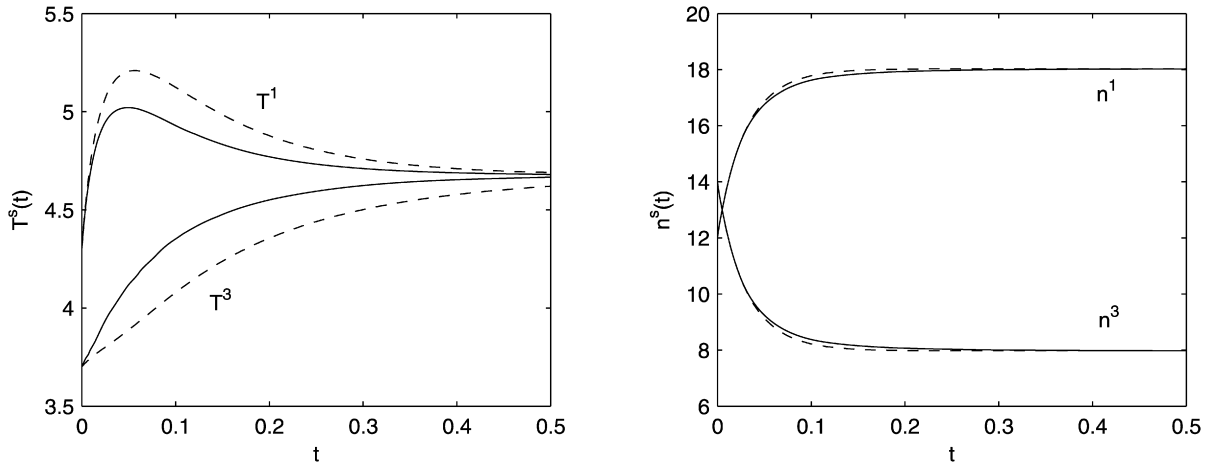

Fig. 4. Left plot: Time evolution of the temperatures T^1 and T^3 obtained by the BGK model (dashed line) an by the DOM model (solid line). Right plot: Time evolution of the number densities n^1 and n^3 obtained by the BGK model (dashed line) and by the DOM model (solid line). The reactive collision frequency exceeds the mechanical one in these pictures.

which is nearly an order of magnitude bigger than the elastic frequencies. As the following results show, this ratio of elastic and reactive collision frequencies is beyond the range of validity of the BGK model. The time evolution of temperatures in Fig. 4 differs significantly for the two methods as expected. However, the differences in the temporal evolution of the number densities are less pronounced. It should be noted that the change of number densities can only be caused by chemical reactions. We observe that the BGK method is still quite good in predicting the chemical reaction rate even in the case of high reaction frequencies, but it is not able to determine accurately the energy transfer due to the chemical reactions and, therefore, to evaluate accurately the temperatures.

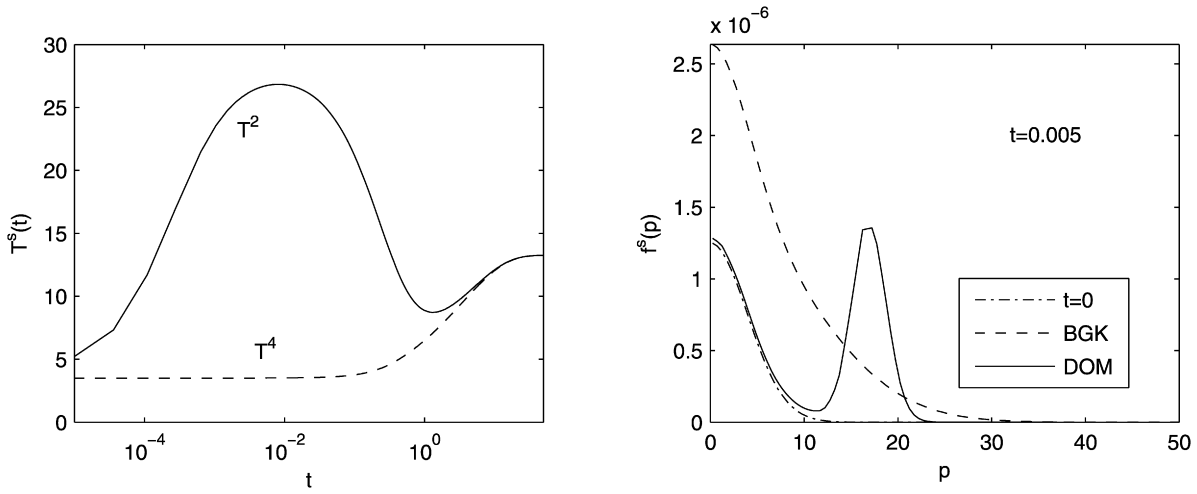

Fig. 5. Left plot: Time evolution of temperatures T^2 and T^4. The results obtained by the DOM and the BGK method coincide. Right plot: The distribution function of species 2 obtained by the DOM and the BGK method at $t = 0.005$ and, for comparison, the initial distribution. Species 2 is initially almost absent in these pictures.

In the following test case, we return to the original initial data but reduce the initial density of species 2 dramatically to

$$n^2(0) = 0.0012 \tag{65}$$

and raise the energy yield to $E_{12}^{34} = 50$. The time evolution of the temperatures of the species 2 and 4 is depicted in the left plot of Fig. 5. Species 1 and 3 behave similarly to species 4 depicted here. The results of DOM and BGK methods coincide, which clearly indicates that the BGK method is also able to reproduce well macroscopic quantities in cases of very different and varying concentrations and high reactive energy yields, if the chemical reaction frequencies are small compared to the elastic ones.

The most striking feature in the left plot of Fig. 5 is the strong increase of the temperature of species 2. This can be explained by the very low initial concentration of this species. The energy released by the chemical reaction is initially carried by the products. In the case of species 2, at the beginning of the relaxation process, a majority of the particles are products of the reaction and carry the additional energy released in the bimolecular reaction. This additional energy causes the strong increase of the temperature in the very initial stage, which becomes evident by investigating the distribution function of species 2. In the right part of Fig. 5, we plotted the distribution functions obtained by DOM and BGK methods at $t = 0.005$. The snapshot is taken at the very fast increase of the temperature of species 2. The distribution function obtained by the DOM method shows that a bump at $p = 18$ is formed by the hot products of the reaction. The rest of the distribution remains virtually unchanged. The BGK method is not able to reproduce this behavior and leads to a completely different distribution, though leading to the same macroscopic quantities, e.g., the correct reaction rates. Later, when the temperature of species 2 decreases, an elastic relaxation towards a local Maxwellian becomes effective.

In our test cases the BGK model does not describe correctly the far from equilibrium distributions even when starting with Maxwellian initial distributions. However, the method can handle arbitrary initial distribution functions as shown in [19] and as confirmed below. Now, we want to demonstrate its performance by studying the bump-on-tail phenomena. To this end, we insert the distributions obtained by the DOM method in the previous test case at $t = 0.005$ as initial conditions into a BGK and DOM calculation. The results are shown in Fig. 6. Although the BGK model can reproduce a similar relaxation pattern as the DOM method, it dramatically underestimates the time scale. The results of the DOM approach show that the bump-on-tail is much more stable as expected from the BGK picture. Although the elastic relaxation finally becomes important, the chemical reaction still rebuilds the bump. Of course, the BGK method cannot reproduce this behavior at a microscopic level, since, by construction, it forces distribution functions towards Maxwellians.

The case of low initial concentration shows that even if the chemical reaction frequency is chosen significantly smaller than every elastic one, it is not always possible to distinguish elastic and chemical relaxation time scales. Of

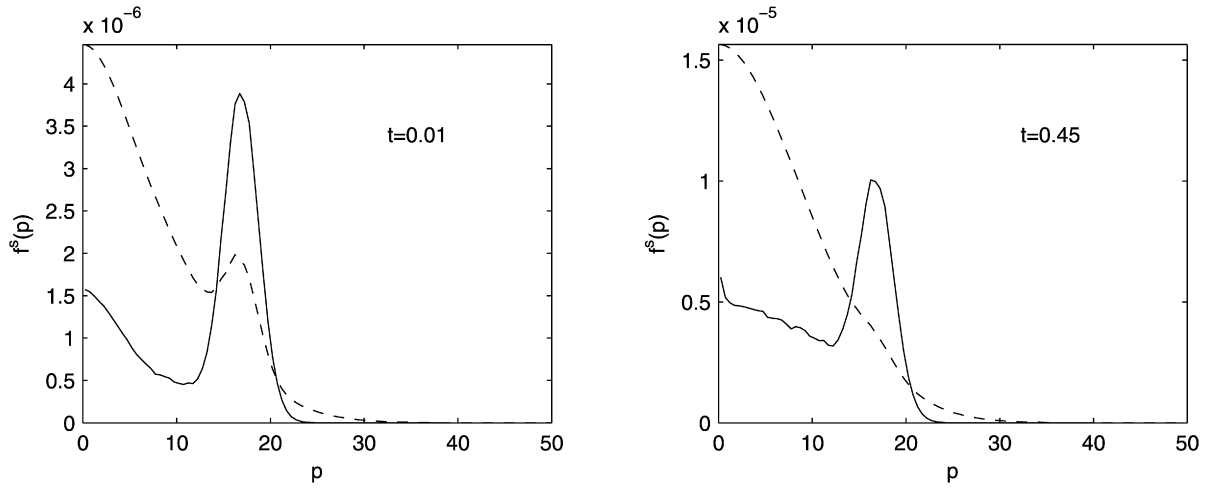

Fig. 6. Distribution function of species 2 obtained by the BGK model (dashed line) and by the DOM methods (solid line) at $t = 0.01$ (left plot) and $t = 0.45$ (right plot). Initial condition is the "bump-on-tail" distribution of Fig. 5.

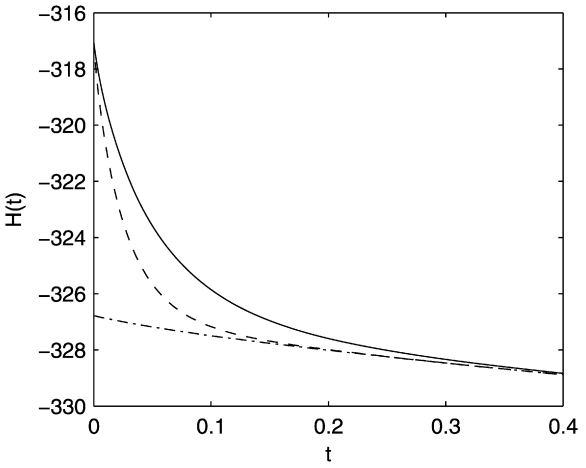

Fig. 7. H-functionals obtained by the DOM (solid line) and the BGK method (dashed line) in the case of tent-shaped initial distributions. The dash-dotted line shows the evolution of the H-functional when starting from a Maxwellian, which coincides for both methods.

course, the long term behavior is solely driven by the chemical reactions and a mechanical equilibrium is reached significantly earlier, but the initial behavior can only be explained as a chemically driven effect. Nevertheless, the BGK method succeeds in accurately describing the time evolution of the main moments of the distribution functions for all species (not shown here for brevity).

In our last test case, we again investigate the effects of non-equilibrium initial distribution functions on the BGK and the DOM calculations. We return to our initial data concerning the macroscopic quantities used in our first study. However, the initial conditions (61) are now relevant to tent functions instead of Maxwellians [19]. We are especially interested in the evolution of the H-functional (27), depicted in Fig. 7. The BGK method predicts a faster decrease of the H-functional than the DOM approach, as expected. In both cases the relaxation of the tent function deviates only at the beginning from the behavior of the H-functional in the case of Maxwellian initial distributions. It should be noted that in the case of initial Maxwellian distributions both methods lead to the same time evolution of the H-functional.

The faster relaxation in the BGK model can also be clearly seen in the distribution functions depicted in Fig. 8. Especially for low momenta, the BGK model overestimates the relaxation rate of the distribution function. This is

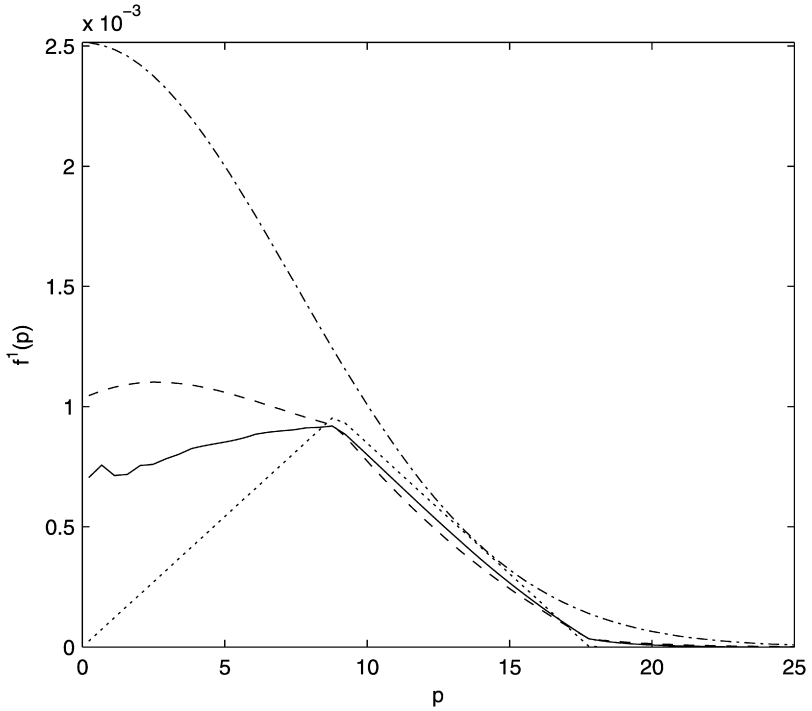

Fig. 8. Tent function as initial distribution for species 1 (dotted line). The equilibrium distributions of species 1 (dash-dotted) obtained by the BGK and DOM method coincide. Distribution functions obtained by the BGK model (dashed line) and by the DOM model (solid line) for species 1 at $t = 0.046$.

not surprising since, due to the special shape of the tent function, the difference between initial and equilibrium distribution is biggest in this area, thus giving a faster relaxation for the BGK model.

6. Conclusion

In this paper we presented an extension of the discrete ordinates method [18] in order to apply it to chemically reacting gases. We made use of the DOM method in comparison with a reactive BGK approach on both macroscopic and microscopic levels. The studies were carried out for the space-homogeneous, isotropic case to reduce computational effort and to make the analysis of distribution functions easier. However, neither of the two methods presented here is limited to this special case, but they can also be applied to more general problems.

Our studies show that the DOM method can reproduce the distribution functions and it is capable of coping with non-equilibrium situations, in contrast to BGK approaches. Although the BGK approximation is unable to predict the distribution functions accurately in the initial transient, the BGK method is an efficient method at a lower computational cost, if one is mainly interested in macroscopic quantities. The computational cost is of course lower for the BGK model than for the DOM calculation, since no evaluation of the conservative collision integral is needed for BGK, just the calculation of moments. This makes the BGK model more competitive in its range of validity.

A possible rule to decide which scheme should be used is based on the ratio between the elastic and the reactive collision frequencies ν_i and ν_{12}^{34}. If ν_i is greater than ν_{12}^{34}, by about one order of magnitude or more, the much cheaper BGK method is adequate and reliable, except for a short initial transient in which its accuracy might be poor if the initial data of the species are very distorted with respect to Maxwellian distributions.

Future works will involve the application of the DOM method to anisotropic and space-dependent problems in order to take full advantage of its capabilities, compared, e.g., to semicontinuous approximations of the kinetic equations [11]. Application to gas kinetic models with other (more realistic) cross sections, which is easy to implement, will also be considered, together with the extension of the DOM method to non-conservative processes, like those occurring in granular materials.

Acknowledgements

This work was performed in the frame of the activities sponsored by MIUR (Project "Mathematical Problems of Kinetic Theories"), by INdAM, by GNFM, and by the University of Parma (Italy), and by the European Network HYKE: "Hyperbolic and Kinetic Equations: Asymptotics, Numerics, Analysis". One author of this article (PL) is grateful to the Department of Mathematics of the University of Parma for the hospitality extended to him during his visits, in which this piece of research was started and completed.

References

[1] A. Nordsieck, B.L. Hicks, Mote Carlo evaluation of the Boltzmann collision integral, in: C.L. Brundin (Ed.), Rarefied Gas Dynamics, Proc. 5th Intern. Symposium on RGD, Plenum Press, New York, 1967, pp. 695–710.
[2] T. Ohwada, Structure of normal shock waves. Direct numerical analysis of the Boltzmann equation for hard-sphere molecules, Phys. Fluids A 5 (1993) 217–234.
[3] S. Kosuge, K. Aoki, S. Takata, Shock-wave structure for a binary gas mixture: finite-difference analysis of the Boltzmann equation for hard-sphere molecules, Eur. J. Mech. B Fluids 20 (2001) 87–126.
[4] L. Pareschi, G. Russo, Numerical solution of the Boltzmann equation I: spectrally accurate approximation of the collision operator, SIAM J. Numer. Anal. 37 (2000) 1217–1245.
[5] G.A. Bird, Molecular Gas Dynamics, Clarendon Press, Oxford, 1994.
[6] R. Gatignol, Théorie cinétique des gaz à répartition discrète des vitesses, Lecture Notes in Physics, vol. 36, Springer-Verlag, Berlin, 1975.
[7] R. Monaco, L. Preziosi, Fluid Dynamic Applications of the Discrete Boltzmann Equation, Series on Advances in Mathematics for Applied Sciences, vol. 3, World Scientific, River Edge, NJ, 1991.
[8] C. Buet, A discrete velocity scheme for the Boltzmann operator of rarefied gas dynamics, in: J. Harvey, G. Lord (Eds.), Rarefied Gas Dynamics, vol. 19, Oxford Science Publication, Oxford, 1995, pp. 878–884.
[9] L. Preziosi, The semicontinuous Boltzmann equation for gas mixtures, Math. Models Methods Appl. Sci. 3 (1993) 665–680.
[10] W. Koller, F. Hanser, F. Schürrer, A semicontinuous extended kinetic model, J. Phys. A 33 (2000) 3417–3430.
[11] W. Koller, A semicontinuous model for bimolecular chemical reactions, J. Phys. A 33 (2000) 6081–6094.
[12] F.G. Tcheremissine, Conservative discrete ordinates method for solving of Boltzmann kinetic equation, in: Ching Shen (Ed.), Rarefied Gas Dynamics, vol. 20, Peking University Press, Beijing, China, 1997, pp. 297–302.
[13] F.G. Tcheremissine, Conservative evaluation of Boltzmann collision integral in discrete ordinates approximation, Comput. Math. Appl. 35 (1998) 215–221.
[14] F.G. Cheremisin, Solving the Boltzmann equation in the case of passing to the hydrodynamic flow regime, Dokl. Phys. 45 (2000) 401–404.
[15] F.G. Tcheremissine, Solution of the Boltzmann equation for arbitrary molecular potentials, in: R. Brun, et al. (Eds.), Rarefied Gas Dynamics, vol. 2: Proceedings of the 21st International Symposium on Rarefied Gas Dynamics, Cepadues-Editions, Toulouse, France, 1999, pp. 173–180.
[16] A. Raines, Study of a shock wave structure in gas mixtures on the basis of the Boltzmann equation, Eur. J. Mech. B Fluids 21 (2002) 599–610.
[17] F.G. Cheremisin, Solution of the Wang–Chang–Uhlenbeck master equation, Dokl. Phys. 47 (2002) 872–875.
[18] F.G. Tcheremissine, Direct numerical solution of the Boltzmann equation, in: M. Capitelli (Ed.), Rarefied Gas Dynamics: 24th International Symposium on Rarefied Gas Dynamics, in: AIP Conference Proceedings, vol. 762, American Institute of Physics, Melville, New York, 2005, pp. 76–81.
[19] M. Groppi, G. Spiga, A Bhatnagar–Gross–Krook-type approach for chemically reacting gas mixtures, Phys. Fluids 16 (2004) 4273–4284.
[20] P.L. Bhatnagar, E.P. Gross, K. Krook, A model for collision processes in gases, Phys. Rev. 94 (1954) 511–524.
[21] P. Welander, On the temperature jump in a rarefied gas, Ark. Fys. 7 (1954) 507–533.
[22] A. Rossani, G. Spiga, A note on the kinetic theory of chemically reacting gases, Physica A 272 (1999) 563–573.
[23] M. Groppi, G. Spiga, Kinetic approach to chemical reactions and inelastic transitions in a rarefied gas, J. Math. Chem. 26 (1999) 197–219.
[24] C. Cercignani, The Boltzmann Equation and its Applications, Springer, New York, 1988.
[25] J.C. Light, J. Ross, K.E. Shuler, Rate coefficients, reaction cross section and microscopic reversibility, in: A.R. Hochstim (Ed.), Kinetic Processes in Gases and Plasmas, Academic Press, New York, 1969, pp. 281–320 (Chapter 8).
[26] P. Andries, K. Aoki, B. Perthame, A consistent BGK-type model for gas mixtures, J. Stat. Phys. 106 (2002) 993–1018.
[27] M. Bisi, M. Groppi, G. Spiga, Grad's distribution functions in the kinetic equations for a chemical reaction, Continuum Mech. Thermodyn. 14 (2002) 207–222.
[28] M. Abramowitz, I.A. Stegun (Eds.), Handbook of Mathematical Functions, Dover, New York, 1965.
[29] N.M. Korobov, The approximate computation of multiple integrals, Dokl. Akad. Nauk SSSR 124 (1959) 1207–1210.
[30] E. Hlawka, Uniform distribution modulo 1 and numerical analysis, Compositio Math. 16 (1964) 92–105.
[31] H. Niederreiter, Existence of good lattice points in the sense of Hlawka, Monats. Math. 86 (1978) 203–219.
[32] N.M. Korobov, Trigonometric Sums and Their Application, Mir, Moscow, 1989.